FABRY-PEROT FIBER-OPTIC TEMPERATURE SENSOR SYSTEM

Margaret L. Tuma
NASA Lewis Research Center

Kristie A. Elam
Gilcrest Electric

Takeo Sawatari, Phil Gaubis, and Yuping Lin
Sentec Corporation

Abstract - In order to monitor aircraft engine performance, there is a need for a sensor which can accurately measure temperature from -50°C to 600°C in an aircraft environment. The objective of the development and testing of this prototype sensor system was to determine the feasibility of operating an optical sensor in such a hostile environment. In this work a photonic sensor was utilized to monitor the exhaust gas temperature (EGT) of an OV-10D aircraft engine. The sensor has successfully flown over 50 hours and proven to be immune to source fluctuations, surface deterioration of the optical element (located inside the sensor head), and able to withstand and operate in normal flight conditions as well as sustained severe flight conditions with forces exceeding 4 g's. Potential commercial uses for this sensor include monitoring temperature for aeropropulsion system control, military vehicle and naval engine control, conventional and nuclear power plant monitoring, and industrial plant monitoring.

INTRODUCTION

Presently, detection over this large temperature range requires multiple photonic sensors whereas this single sensor system is capable of detecting temperature over the entire range. For future supersonic and hypersonic aircraft, there is a need for high performance as well as safe sensors for aircraft engine control. Photonic sensors meet this need and have several benefits over conventional electronic sensors for aircraft applications. These benefits include immunity to electromagnetic interference, larger bandwidth, as well as providing a safety advantage due to the lack of a sparking hazard. In contrast, conventional electronic sensors such as thermocouples, thermistors, and bi-metal type devices are susceptible to electromagnetic interference, require shielding, and possess a sparking safety hazard.

Optical temperature measurement techniques have been studied in the past and can be characterized into three categories based upon their signal generation method. These categories include: [1]

1) optically emissive, thermally powered
2) optically emissive, optically powered
3) non-emissive, optically powered.

An advantage of optically emissive, thermally powered sensors is that they do not require an optical light source. These fiber-linked blackbody emitters are generally used to detect high temperatures (>600°C) [2]. Optically emissive, optically powered sensors require an excitation light source. A typical optically emissive, optically powered sensor is a fluorescence time rate of decay sensor [3]. An advantage of this sensor is the lack of sensitivity to source fluctuations whereas disadvantages include complex data reduction, large insertion loss, particularly at the quench point of the fluorescent material, and limited temperature range. Further disadvantages of the two sensor types just described include lack of measurement stability, short lifetimes, and inadequate dynamic range. The sensor system studied in this research is a non-emissive, optically powered sensor where changes in temperature are wavelength encoded onto the spectrum of a white light source. This wavelength encoding is achieved by utilizing a Fabry-Perot interferometer as the sensor transducer. Previous Fabry-Perot type temperature sensors have utilized a thin film coating as the etalon [4-5], which limits the temperature range to approximately 300°C due to surface adhesion problems. Other Fabry-Perot temperature sensors have utilized sapphire fiber to detect higher temperatures, but are mainly single-mode devices [6-7].

THEORY

A broadband photonic temperature sensor system has been constructed utilizing a Fabry-Perot interferometer as the sensing mechanism [8]. The present sensor, shown in Figure 1, consists of an optical cavity, d,

between a piece of reflecting metal and the end of an optical sapphire fiber. Light enters the optical sapphire fiber via the SMA connector. A small portion of the incident light is reflected at the distal end of the sapphire fiber (~4%) and the remaining light is incident upon the metal reflector. Light reflected off the metal surface (~90%) re-enters the fiber and propagates back to the SMA optical connector. These two reflected beams interact to produce interference fringes. As the sensed temperature varies, the distance between the metal reflector and fiber, d, varies due to thermal expansion and contraction of the sensor housing and sapphire fiber. This thermal property is exploited to deduce temperature by interrogating the sensor with broadband light and analyzing the modulated spectrum [8]. The number of fringes in this reflected spectrum increases with increasing temperature.

The sensor is wavelength modulated as opposed to intensity modulated. Hence, it is expected to be immune from power fluctuations of the source, fiber bends, changes in the reflectivity of the metal reflector due to oxidation, and changes in the spectrometer's sensitivity.

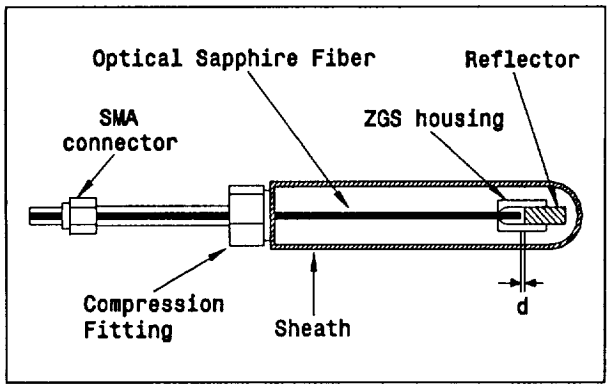

Figure 1: Schematic drawing of sensor head.

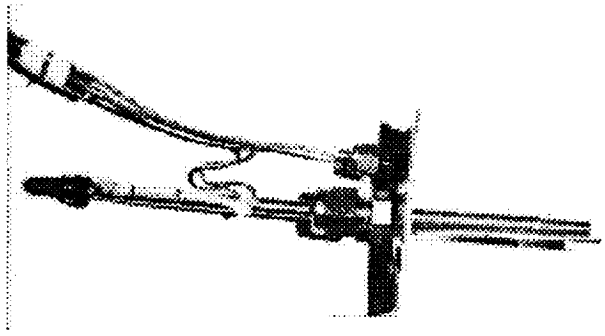

Figure 2: Photograph of sensor assembly.

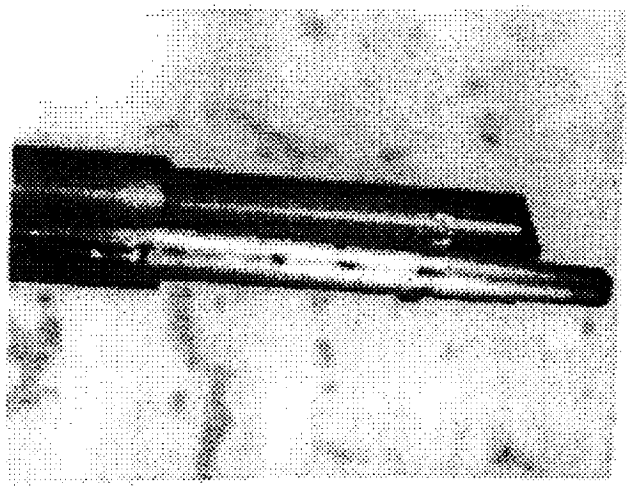

Figure 3: Close-up photograph of sensor tip.

EXPERIMENTAL SETUP

The photonic sensor was fabricated by Sentec Corporation [9] and is shown in Figures 1 and 2. The prototype sensor assembly is approximately 6" long with an outer diameter of 0.19". Light enters the sensor via an SMA optical connector, located on the left side of Figure 1, and propagates down the sapphire optical fiber, located inside the inconel sheath. The opposite end of the sapphire fiber is optically polished and inserted into a ZGS (platinum alloy) housing in close proximity to a ZGS reflector. Interference between the two beams, the beam reflected at the fiber tip and the beam reflected off the metal reflector, produces interference fringes. Because the thermal expansion coefficients of sapphire and ZGS are different, the distance between the fiber end and the reflector, d, changes with temperature. Here, high temperature cement was used to bond the sapphire fiber to the ZGS housing, which was found sufficient for preliminary testing. However, another bonding technique will be utilized in future work.

As shown in Figure 2, a type K thermocouple is attached directly to the sensor by three spot-welded metal tie wraps. A close-up photograph of the sensor head and thermocouple is shown in Figure 3. A thermocouple is not suitable for long term use in this harsh environment. Due to its lack of rigidity, a thermocouple requires constant visual inspection and more frequent replacement than the optical sensor. As shown by the photograph in Figure 4, and the schematic drawing in Figure 5, the portion of the sensor to the right of the mounting plate was installed inside the exhaust duct of the aircraft. In Figure 4, the sensor is located at

approximately ten o'clock, as indicated by the arrow. The vertical lines are the tail pipe vanes used to direct airflow, the region inside the inner diameter is the exhaust duct, and the outer metal surface is the shroud. As shown in Figure 5, the mounting plate is affixed to the shroud, with the sensing portion penetrating into the exhaust region. Here, the maximum temperature observed was approximately 600°C.

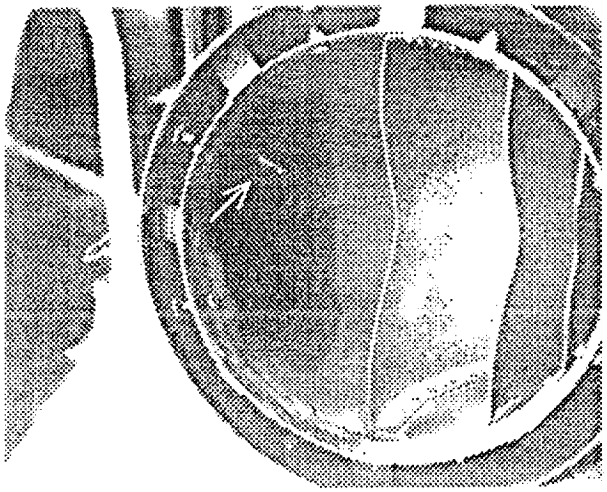

Figure 4: Sensor installed in exhaust duct of an OV-10D airplane.

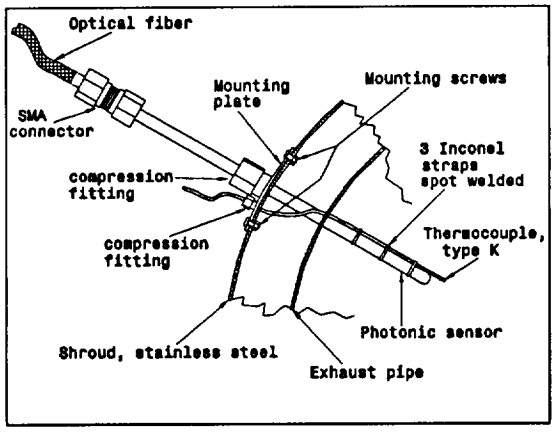

Figure 5: Cross section schematic of sensor mount.

The sensor system, shown in Figure 6, consists of a white light source (Ocean Optics LS-1), a 300 micron core optical 2 x 1 coupler (Gould CA-300-50-12-13-07-1), an SMA connector, 15 feet of 320 micron core multimode optical cable (TCL-MB320H), the photonic sensor (Sentec), 3 type K thermocouples, a spectrometer card (Ocean Optics PC-1000) which could detect optical wavelengths from 500-1000 nm, an eight channel thermocouple card (Omega OMD-5508TC), and a Syscom Pentium computer.

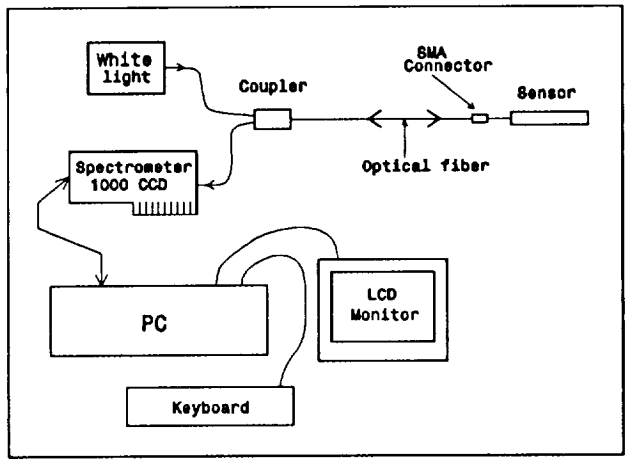

Figure 6: Photonic temperature sensor system.

As illustrated in Figure 6, output from the white light source is coupled into one arm of a 2 x 1 optical coupler. This light enters the sensor's optical sapphire fiber via an SMA optical connector. It was necessary to use high temperature sapphire fiber because silica fiber would degrade at the elevated flight test operating temperatures. The only disadvantage of using the sapphire fiber is its large optical attenuation, which did not prove to be a problem.

Referring again to Figure 6, light reflected from the metal surface is coupled out of the sensor via the SMA connector and travels through the 15 foot multimode fiber into the 2 x 1 coupler. This light continues into the opposite coupler leg which directs approximately 50% of the reflected light to the rear-mounted SMA connector on a computer plug-in spectrometer card. The data acquisition Pentium computer and white light source were located in the cargo area of the plane. Care was taken to minimize the number of bends in the optical fiber and maximize the bend radius of each bend. Using a single fiber to interrogate the sensor and transmit the modulated signal has several advantages, including increased reliability and reduced production cost. This 1000 pixel CCD linear array has a resolution of 1 nm over the 500 to 1000 nm range and is capable of recording a single spectrum in a few milliseconds. The modulated light is incident upon the spectrometer card which converts the optical spectral data into an electrical signal. Due to the vibration of the plane, it was

determined that a hard disk was likely to fail during flight tests. Therefore, data was saved to a floppy disk. This limited the data acquisition rate to approximately 1 spectral reading every 20 seconds, due to the limited storage capacity of the floppy disk.

In the exhaust sensing region, the maximum temperature observed was approximately 600°C. A photograph of the installed sensor and thermocouples as viewed through the tail pipe access panel is shown in Figure 7. Three type K thermocouples interfaced to the data acquisition computer were used to monitor the sensor system. As previously shown in Figure 3, the first thermocouple was attached directly to the sensor head to validate its performance. The second thermocouple was attached to the outside of the exhaust duct to monitor the heat transfer from the sensor patch hole. For health monitoring purposes it was necessary to observe the SMA connector temperature because failure would occur at temperatures exceeding 125°C. Therefore, the third thermocouple was welded to the base of the SMA connector.

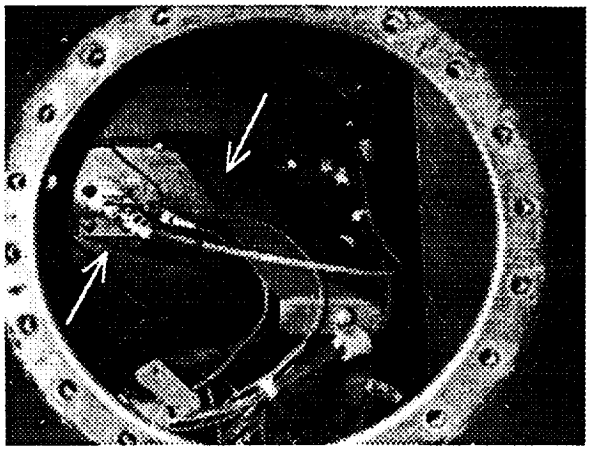

Figure 7: Installed sensor and thermocouples.

During the initial ground tests, the sensor was attached to the exhaust duct via the 4 mounting screws on the bracket shown in the left of Figure 7. However, the sensor was found to vibrate excessively and in preliminary tests, a spot weld on the sensor housing weakened and eventually failed. Therefore it was determined that (1) the sensor portion external to the shroud required a brace and (2) the spot weld required reinforcement. As shown in Figure 7, plastic tubing was placed around the sensor/fiber connection to reduce vibration. To further dampen the vibration at this connection, a brace was used to support a portion of the 15 foot optical fiber. Regarding the weld, a diagram of the sensor prior to the laser weld is shown in Figure 8.

As shown in Figure 9, a bead of nickel was placed over the original spot weld and then laser-welded. This greatly improved the strength and durability of the sensor housing.

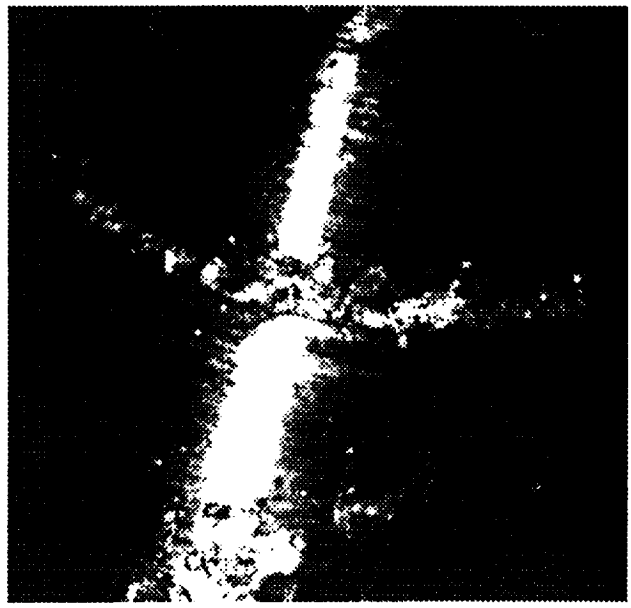

Figure 8: Sensor prior to laser weld.

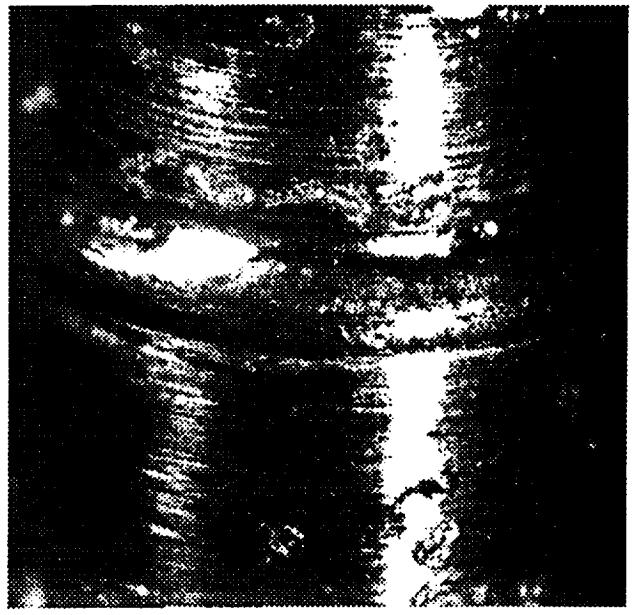

Figure 9: Sensor after laser weld.

SENSOR CALIBRATION

A calibration was required and performed prior to the flight tests. Ideally, the sensor would be installed and calibrated in its operating environment, however, in this case that was not possible. To characterize the temperature profile of the exhaust region, thermocouples were placed in various regions. Preliminary tests indicated that the exhaust region did not exceed 600°C while the area near the SMA connector did not exceed 90°C. Therefore, to simulate the environment the sensor would experience during flight tests, the sensor was placed in the top exhaust duct of an NEY 6-135A programmable oven with the sensing portion protruding into the furnace, as shown in Figure 10. The sensor was mounted on a large piece of brass, which served as a heat sink, similar to the exhaust pipe shroud on the plane. This allowed the SMA area to remain cool while the sensing portion was exposed to the high temperature in the furnace.

An automated calibration was performed which took 3 days. A calibration from room temperature to 600°C was performed. The furnace temperature increased at a rate of approximately 0.16°C/minute. A total of 117 reflected spectra were taken every 35 minutes. This corresponded to roughly 5°C increments in sensor temperature, based upon the output of the thermocouple attached to the sensor. Each of the 117 spectra was saved to a computer data file to be used during the flight tests.

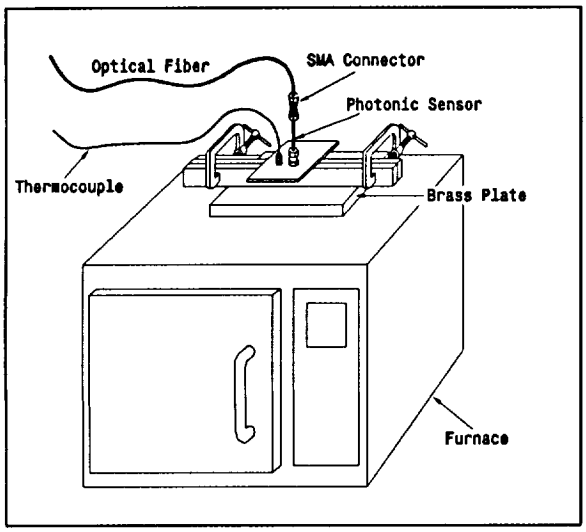

Figure 10: Calibration furnace setup.

DATA ACQUISITION - PROCEDURE

The temperature of the exhaust duct was nearly 20°C prior to each day's initial flight. Approximately 1 hour prior to engine start-up, the optical SMA connectors were cleaned and reconnected using a small amount of Cargille index matching fluid. At the same time, the light source was powered and allowed to warm up in order to reduce source fluctuations and electronic drift. After the 1 hour warm-up time, a reference spectrum was taken. On a few occasions when more than 1 test flight was scheduled on a given day, the exhaust duct did not cool down to 20°C and therefore a new reference spectrum could not obtained for the subsequent flight. On these occasions, the same reference spectrum was used for both flights. This was not an optimum condition for the prototype system, causing the sensor's performance to be moderately degraded. In one case, the average difference between the thermocouple temperature and the sensor temperature was 4.8°C and 8.8°C, with a standard deviation of 9.3°C and 11.7°C, for the first and second flight, respectively.

Just prior to engine start-up, external power was removed from the plane. Without power to the light source and computer, it was not possible to monitor the exhaust temperature. Approximately one minute after engine start-up, aircraft power was initiated. Once this occurred, the sensor system began acquiring optical spectra and calculating the exhaust temperature every 20 seconds.

Sensor performance was monitored by a flight test engineer during each test by viewing the sensor output and thermocouple readings on an LCD monitor. The most significant problem encountered during 4 particular flights was loosening of the SMA connector. To eliminate this problem, safety-wire was utilized. However, it fatigued the SMA connector and was discontinued. It was determined that the sensor connector could be tightened sufficiently to eliminate this problem. A commercial version of this sensor would transfer the optical connection to a more stable location and/or utilize a different type of optical connector.

DATA REDUCTION

Data is normalized by dividing the raw reflected spectra by the reference spectrum, taken prior to each flight. At room temperature, the normalized spectrum is nearly a straight line. As the sensed temperature increases, the normalized spectra becomes sinusoidal in appearance with increasing numbers of fringes. Each sensed temperature is associated with a particular reflected spectral curve. Figure 11 illustrates a typical high temperature spectrum.

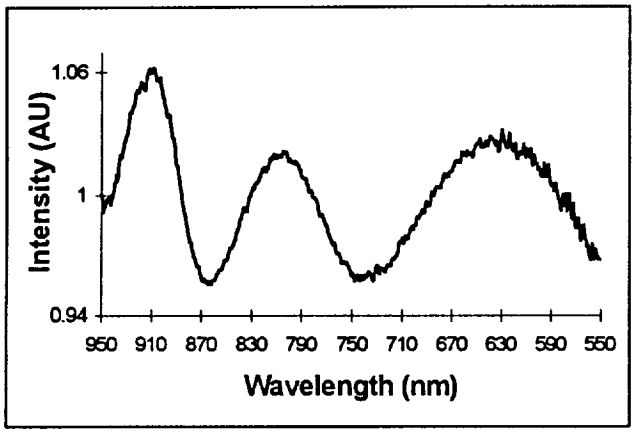

Figure 11: Typical spectrum reflected from sensor exposed to high temperature.

Temperature is deduced by comparing the normalized spectrum to each of the 117 calibration curves, which are stored in a look-up table. The computer algorithm calculates the minimum squared difference between the current fringe pattern and the set of calibration curves. However, the temperature corresponding to this minimum is accurate only to within the 5°C calibration increment. In order to more precisely determine the temperature, a parabolic approximation is used: a parabolic curve which fits three points around the minimum is determined and the minimum of the parabolic curve is defined as the measured temperature.

RESULTS

Over 50 hours of flight tests were successfully completed consisting of 40 flights. The flight profiles for the first 20 flight test hours were straight and level. After 20 hours, the flight profiles were much more severe, exposing the sensor to forces exceeding 4 g's when performing maneuvers. These maneuvers consisted of loops, aileron rolls, Cuban Eights, Barrel Rolls, hard turns with 90 degree angle of bank, and touch and go landings.

As expected, the calibration was determined to be a critical factor in the sensor's performance. During initial flight tests, it became apparent that the computer algorithm consistently calculated incorrect temperatures in the 475°C to 525°C temperature range. Upon further investigation it was discovered that during calibration the furnace had rapidly increased its temperature by 30°C between two calibration readings instead of the expected 5°C interval. This jump discontinuity is shown in Figure 12 and indicated by the arrow. To remedy this, a new calibration was performed, also shown in Figure 12. Flight test data analyzed using the old calibration was re-analyzed using the new calibration with significant improvement in results. Figure 13 shows flight test data analyzed using the two calibrations.

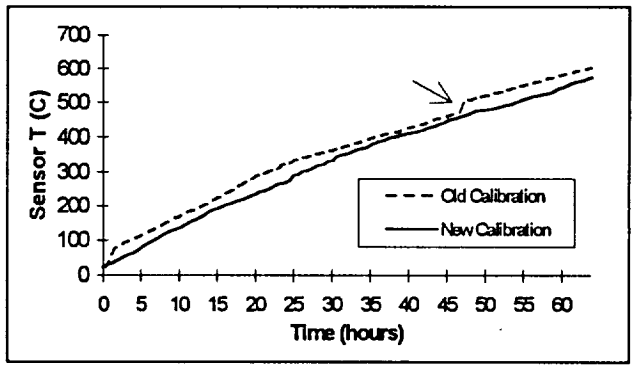

Figure 12: Comparison of old and new calibrations.

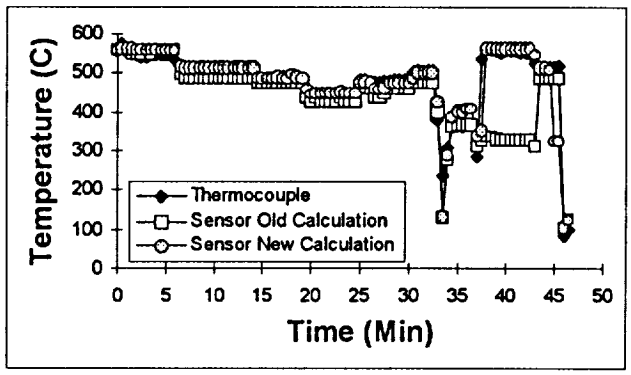

Figure 13: Comparison of sensor data analyzed using the old and new calibrations.

Calculated temperature vs. thermocouple readings for a few of the flight tests are shown in Figures 13-15. Figure 13 illustrates the temperature results for a flight profile with varied engine power levels. Figure 14 illustrates the temperature results for a typical straight

and level flight profile, and Figure 15 for a flight where maneuvers were performed. Based on these flight test results, the photonic sensor appears to have accurately detected the exhaust gas temperature.

The average difference between the thermocouple output and the sensor output and standard deviations of the three flights are given in Table 1. The straight and level flight profile produced the most accurate results because the sensor was in near equilibrium throughout the flight. Flight test profiles with varied engine power settings produced less accurate temperature results, while the flight profiles that included maneuvers yielded the highest errors. Due to its thermal mass, the temperature sensor exhibited a slower response to temperature change than expected. The time constant, τ, was approximately 1 minute. This slow response to temperature change appears to be the cause of increased errors for the flight tests profiles with varied power settings and maneuvers.

Figure Number	Average T difference	Average Std. Dev.	Flight Profile
Figure 14	4.5°C	9.3°C	Straight
Figure 13	7.5°C	12.8°C	Varied
Figure 15	9.8°C	19.8°C	Maneuvers

Table 1: Statistical analysis of three flights.

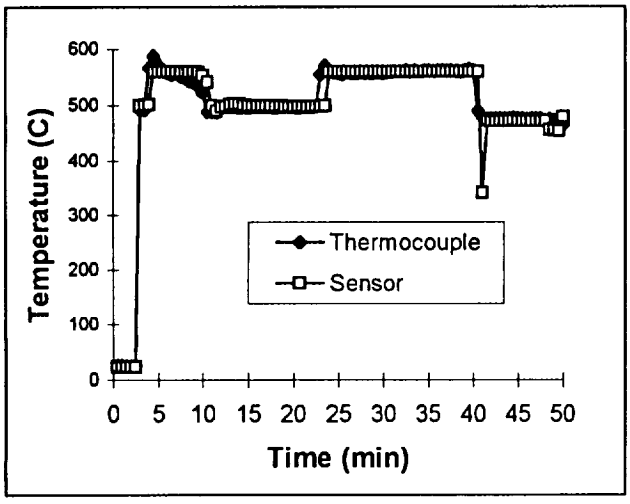

Figure 14: Flight test results for a straight and level flight.

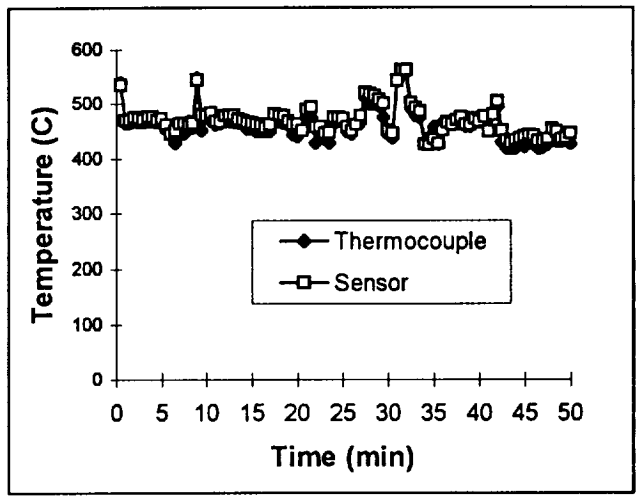

Figure 15: Flight test results for a flight with maneuvers.

SUMMARY

Ground and flight tests performed on an OV-10D airplane verified the prototype sensor system's operation and demonstrated the feasibility of utilizing such a system in the harsh environment of an airplane exhaust. For a prototype system, the sensor performance exceeded expectations. The sensor system successfully operated over 50 flight hours which consisted of straight and level flights in addition to varied engine power settings, maneuvers, and touch and go landings. These tests proved that it is feasible to operate such a photonic sensor system in the hostile environment of an aircraft engine exhaust.

FUTURE WORK

In the future, data acquisition will be improved to reduce the amount of time between data points, which is presently 20 seconds. Methods to accomplish this include: utilizing an electronic chip to store the calibration spectra in a lookup table, utilizing an electronic chip to determine the best match to the present spectrum, and writing smaller data files to the floppy disk. Presently, the entire spectrum is saved, whereas to increase the data acquisition rate, only the calculated temperature need be saved.

Plans are under way to improve the bond between the sapphire fiber and the sensor housing using a gold braze instead of the high temperature cement. This will improve sensor performance and reliability. The next sensor will be much smaller in size to decrease its response time to temperature change. To alleviate the optical connection from loosening, the SMA connector

may be replaced with a more rugged connector. Lastly, to improve sensor resolution, calibration data may be acquired in 2°C increments.

ACKNOWLEDGMENTS

The authors wish to thank Rich Ranaudo, William Rieke, and Larry Schultz for piloting the plane during the sensor flight tests, Bud Schutte for maintaining the airplane and installing the sensor system, Mike Perez for assisting in the sensor installation, Ed Emery and Steve Plaskon for coordinating the installation of the associated electronic components, Mike Ernst for design of the sensor vibration-damping mount, George Saad for welding the thermocouples to the sensor and reinforcing the sensor welds, Jih-Fen Lei for the use of her programmable furnace, and Amanda Emmel for the statistical analysis of the flight test data.

REFERENCES

[1] Beheim, G., "Optical Temperature Sensors", in *Integrated Optics, Microstructures, and Sensors*, pp. 285-313, 1995.

[2] Milcent, E., et. al. "Influence of High Temperatures on a Fiber-Optic Probe for Temperature Measurement," Appl. Opt., Vol. 33, No. 25, pp. 5882-5887, 1994.

[3] Tilstra, S.D., "A Fluorescence-Based Fiber Optic Temperature Sensor For Aerospace Applications." Specialty Fiber Optic Systems for Mobile Platforms, Proc. SPIE, Vol. 1589, pp. 32-37, 1991.

[4] Beheim, G., Sotomayor, J.L., Tuma, M.L., and Tabib-Azar, M., "Fiber-Optic Temperature Sensor Using Laser Annealed Silicon Film," SPIE Proceeding, Vol. 2291, pp. 92-98, 1994.

[5] Schultheis, L. Amstutz, H., Kaufmann, M., "Fiber-optic temperature sensing with ultrathin silicon etalons," Opt. Lett, Vol. 13, No. 9, pp. 782-784, 1988.

[6] Wang, A., Gollapudi, S., Murphy, K. A., May, R., Claus, R. O., "Sapphire-fiber-based intrinsic Fabry-Perot interferometer," Op. Lett. Vol. 17, No. 14, pp. 1021-1023, 1992

[7] Wang, A., Gollapudi, S., May, R. G., Murphy, K. A., Claus, R. O., "Advances in sapphire-fiber-based intrinsic interferometric sensors," Opt. Lett. Vol.. 17, No. 21, pp.1544-1546, 1992.

[8] Sawatari, T., Gaubis, P., Mattes, B., Charnetski, C., "Fiber Optics Temperature Sensor," Invited Paper, SPIE Proceeding, Vol. 2686, pp. 132-145, 1996.

[9] Sentec Corporation fabricated the sensor as part of an SDB contract with NASA Lewis Research Center (NAS3-27202).

REPORT DOCUMENTATION PAGE

Form Approved
OMB No. 0704-0188

1. AGENCY USE ONLY (*Leave blank*)	2. REPORT DATE	3. REPORT TYPE AND DATES COVERED
	September 1997	Technical Memorandum

4. TITLE AND SUBTITLE

Fabry-Perot Fiber-Optic Temperature Sensor System

5. FUNDING NUMBERS

WU-519-20-53-00

6. AUTHOR(S)

Margaret L. Tuma, Kristie A. Elam, Takeo Sawatari, Phil Gaubis, and Yuping Lin

7. PERFORMING ORGANIZATION NAME(S) AND ADDRESS(ES)

National Aeronautics and Space Administration
Lewis Research Center
Cleveland, Ohio 44135-3191

8. PERFORMING ORGANIZATION REPORT NUMBER

E-10934

9. SPONSORING/MONITORING AGENCY NAME(S) AND ADDRESS(ES)

National Aeronautics and Space Administration
Washington, DC 20546-0001

10. SPONSORING/MONITORING AGENCY REPORT NUMBER

NASA TM-113172

11. SUPPLEMENTARY NOTES

Prepared for the 17th International Congress on Instrumentation in Aerospace Simulation Facilities sponsored by the Naval Postgraduate School, Monterey, California, September 29—October 2, 1997. Margaret L. Tuma, NASA Lewis Research Center; Kristie A. Elam, Gilcrest Electric, Cleveland, Ohio; Takeo Sawatari, Phil Gaubis, and Yuping Lin, Sentec Corporation, 2000 Oakley Park Rd., Suite 205, Walled Lake, Michigan 48390 (work performed under NASA Contract NAS3-27202). Responsible person, Margaret L. Tuma, organization code 5520, (216) 433-8665.

12a. DISTRIBUTION/AVAILABILITY STATEMENT

Unclassified - Unlimited
Subject Category 74

This publication is available from the NASA Center for AeroSpace Information, (301) 621-0390.

12b. DISTRIBUTION CODE

13. ABSTRACT (***Maximum 200 words***)

In order to monitor aircraft engine performance, there is a need for a sensor which can accurately measure temperature from -50°C to 600°C in an aircraft environment. The objective of the development and testing of this prototype sensor system was to determine the feasibility of operating an optical sensor in such a hostile environment. In this work a photonic sensor was utilized to monitor the exhaust gas temperature (EGT) of an OV-10D aircraft engine. The sensor has successfully flown over 50 hours and proven to be immune to source fluctuations, surface deterioration of the optical element (located inside the sensor head), and able to withstand and operate in normal flight conditions as well as sustained severe flight conditions with forces exceeding 4 g's. Potential commercial uses for this sensor include monitoring temperature for aeropropulsion system control, military vehicle and naval engine control, conventional and nuclear power plant monitoring, and industrial plant monitoring.

14. SUBJECT TERMS	15. NUMBER OF PAGES
Optical fiber; Fabry-Perot; Temperature; Sensor; White-light	10
	16. PRICE CODE: A02

17. SECURITY CLASSIFICATION OF REPORT	18. SECURITY CLASSIFICATION OF THIS PAGE	19. SECURITY CLASSIFICATION OF ABSTRACT	20. LIMITATION OF ABSTRACT
Unclassified	Unclassified	Unclassified	